Journal of Solid State Chemistry 184 (2011) 1571–1575

Contents lists available at ScienceDirect

Journal of Solid State Chemistry

journal homepage: www.elsevier.com/locate/jssc

Rapid Communication

Preparation and drug release behavior of temperature-responsive mesoporous carbons

Xiufang Wang [a], Ping Liu [b], Yong Tian [a,*]

[a] College of Pharmacy, Guangdong Pharmaceutical University, Guangzhou 510006, China
[b] School of Chemistry and Chemical Engineering, Henan Institute of Science and Technology, Xinxiang 453003, China

ARTICLE INFO

Article history:
Received 26 January 2011
Received in revised form
5 April 2011
Accepted 9 April 2011
Available online 19 April 2011

Keywords:
Ordered mesoporous carbons
Temperature-responsive
Controlled release

ABSTRACT

A temperature-responsive composite based on poly (N-isopropylacrylamide) (PNIPAAm) and ordered mesoporous carbons (OMCs) has been successfully prepared by a simple wetness impregnation technique. The structures and properties of the composite were characterized by infrared spectroscopy (IR), X-ray diffraction (XRD), transmission electron microscopy (TEM), N_2 sorption, thermogravimetric analysis (TG) and differential scanning calorimetry (DSC). The results showed that the inclusion of PNIPAAm had not greatly changed the basic ordered pore structure of the OMCs. Ibuprofen (IBU) was selected as model drug, and in vitro test of IBU release exhibited a temperature-responsive controlled release delivery.

1. Introduction

Recently, poly (N-isopropylacrylamide) (PNIPAAm) has been of great interest because it was widely used as "smart materials" for controlled drug release. It was well-known that PNIPAAm was a temperature responsive polymer and could undergo a hydrophilic–hydrophobic transition at a "lower critical solution temperature (LCST)" (about 32 – 34 °C) [1]. There have been a number of reports on the preparation and controlled drug release of PNIPAAm/mesoporous silica composites [2–9].

However, the surface silanol for mesoporous silica materials might produce interactions with drug molecules such as cytochrome c and lysozyme, which might lead to the loss of drug activity [2,3]. Indeed, studies on bio-encapsulation of proteins in organically modified silica glasses (with pores of 4–10 nm) have shown that the surface modification of the silica-based host matrix with hydrophobic organic groups enhanced the protein helicity and consequently, its biological activity [2]. Menaa et al. [3] showed also the influence of the siloxane network [–Si–O–Si–] on the protein secondary structure, demonstrating via MAS 29Si NMR that the content of silanol group forming the structure of the host matrix was an unfavorable factor for protein helicity (i.e. biological activity). In addition, the structural stability of the mesoporous silica adsorbent after adsorption was relatively poor due to the hydrolysis of their siloxane bridges [10,11]. Ordered mesoporous carbons (OMCs) have shown great potential applications as drug release carriers because of their well-ordered pore structure, very high specific pore volume, specific surface area, tunable pore diameter and biocompatibility [12–17]. Moreover, they are highly tolerant in aqueous environment compared with silica materials. Researches on the use of mesoporous carbon for drug release were very interesting indeed for their hydrophobicity and the generated regular pore size distribution.

To our knowledge, the temperature-responsive organic–inorganic composite based on the OMCs in this study was reported for the first time. The microstructures of PNIPAAm/OMCs composite were investigated by XRD, TEM, N_2 sorption and IR. IBU, as an anti-inflammatory drug, has poor water solubility (2.3 mg/ml at pH7.4) and was commonly used as the release drug model [18], due to its good pharmacological activity and small molecule size (~1 nm), which could fit easily into the pores of OMCs. The release process was monitored by UV–vis spectroscopy.

2. Materials and methods

2.1. Synthesis of OMCs

OMCs were synthesized by a similar procedure [19]. Typically, 1.0 g of AlSBA-15($AlCl_3$ incorporated in ordered siliceous SBA-15 templates[20]) was infiltrated with 2.0 ml of FA (furfuryl alcohol, Tingxin Chemical Regent of Shanghai) by incipient wetness at room temperature. The composite thus prepared was heated at 80 °C for 12 h under vacuum for the polymerization of FA and then at 150 °C for 6 h. After cooling to room temperature, the

* Corresponding author. Fax: +86 2039352129.
E-mail address: fengshoutian@hotmail.com (Y. Tian).

0022-4596/$ - see front matter Crown Copyright © 2011 Published by Elsevier Inc. All rights reserved.
doi:10.1016/j.jssc.2011.04.019

sample was heated to 300 °C (1 °C/min), then to 850 °C (5 °C/min) and kept the pyrolysis step for 4 h under flowing argon atmosphere (200 ml/min). The obtained black powders were washed with HF (20%), filtered and washed with water repeatedly until the pH value was close to 7 and then washed with ethanol. Finally, the sample was dried under vacuum at 40 °C for 24 h.

2.2. Synthesis of PNIPAAm/OMCs composite

For the synthesis of PNIPAAm/OMCs composite, a simple wetness impregnation technique was employed to introduce monomer into the mesoporous carbon material. Briefly, 0.2 g of N-isopropylacrylamide (NIPAAm, Aldrich), 0.01 g of N, N′- methylenebisacrylamide (BIS, Fluka) and 0.005 g of initiator azobisisobutyronitrile (AIBN, Aldrich) were dissolved in 2 ml of acetone by sonication. 0.4 g of the as-prepared carbon was impregnated with the solution, and the solvent was removed under vacuum at room temperature. 0.2 g of water was added to the mixture in the flask. The mixture was kept under a nitrogen atmosphere in order to remove oxygen and was placed in an oil bath preset at 70 °C for 24 h. The obtained product was soaked in methanol for 24 h. The product was isolated by filtration, washed with methanol and dried under vacuum at 40 °C for 6 h. The obtained composite powder was named as PNIPAAm/OMCs.

2.3. Loading and in vitro IBU release

0.25 g of PNIPAAm/OMCs composite was added into 50 ml of IBU solution in hexane (35 mg ml^{-1}), followed by stirring at 45 °C for 24 h in a closed batch to prevent the evaporation of hexane. The loaded materials were then filtered and dried under vacuum at 40 °C for 12 h. The sample was named as PNIPAAm/OMCs-IBU. 20 mg of PNIPAAm/OMCs-IBU was immersed into 50 ml of simulated body fluid (SBF, pH=7.4) [21,22] at 37 °C under stirring at 100 rpm. Syringe filters were used to avoid interference from suspended scattering particles in the UV–vis analysis. 3 ml of sampling was extracted at given time intervals, diluted properly with SBF, and analyzed by UV–vis spectroscopy at a wavelength of 272 nm. The volume removed was complemented with the same amount of preheated SBF. The experiments were carried out in triplicate. The content of IBU in the composite was determined by thermogravimetric (TG) analysis.

2.4. Characterization

The XRD patterns were recorded on a Multi-Purpose Diffractometer (PANanalytical. Inc. X'Pert Pro., MPD) with Cu *K*R radiation (0.1540 nm), using an operating voltage of 40 kV and 40 mA, 0.017° step size and 4.96 s step time. Microscope glass slides were used as sample supports. The samples were manually ground prior to the XRD analysis and all measurements were performed at room temperature. Nitrogen adsorption isotherms were measured with Micromeritics Tristar 3020 volumetric adsorption analyzer at −196 °C. The calcinated carbon sample was degassed at 200 °C for 4 h prior to the measurements. The PNIPAAm/OMCs composite was degassed at 100 °C for 10 h. The specific surface area of the samples was calculated using the BET method. The pore size distributions were derived from the adsorption branches of isotherms using the Barett–Joyner–Halenda (BJH) model, and the total pore volumes (V_t) were estimated from the adsorbed amount at a relative pressure p/p_0 of 0.99. TEM experiments were conducted on a JEOL 2011 microscope operated at 200 kV. The samples for TEM measurements were suspended in ethanol and supported onto a holey carbon film on a Cu grid. Differential scanning calorimetry (DSC) and thermogravimetric (TG) analysis were performed on a STA449C thermal analyzer under N_2 flow with a heating rate of 2 and 10 °C/min, respectively. Infrared (IR) spectra were obtained on a Nicolet360 spectrometer using the KBr pellet technique. The UV–vis absorption spectra values were measured on a U-3010 spectrophotometer.

3. Results and discussion

The bands at 1650 and 1549 cm^{-1} could be assigned to C=O stretching and N–H bending vibrations for polymer PNIPAAm, respectively (Fig. 1a) [8]. The bands located at 1388 and 1369 cm^{-1} were due to isopropyl group, and the band at 1459 cm^{-1} was related to the bending vibration of C–H (Fig. 1a) [23,24]. In addition, little shifts of C=O and N–H bands compared to the pure PNIPAAm were also observed (Fig. 1b), indicating a weak interaction between the polymer and carbon material. For the PNIPAAm/OMCs composite, the characteristic bands of polymer were still observed besides those for carbon materials and the bands at around 1585 cm^{-1} and a broad band at about 1100 cm^{-1} were characteristics for the carbon materials(Fig. 1c) [25]. These results could be a proof that the PNIPAAm has been incorporated into the carbon material.

Small-angle XRD pattern of the pure carbon was shown in Fig. 2a. The carbon sample showed three well-resolved XRD peaks with a strong (1 0 0) reflection at a low angle and two small peaks at higher angles, which can be indexed into 100, 110 and 200 reflections, indicating a good structural quality of the carbon material and the patterns can be assigned to an ordered structure of hexagonal symmetry with *p6mm* space group [20,26]. The highly ordered structure was further proved by TEM images (Fig. 3a).

Small-angle XRD pattern of the PNIPAAm/OMCs composite was exhibited in Fig. 2b. The three main XRD peaks were still observed, showing that the hexagonal mesopores of the carbon material were stable after the inclusion of PNIPAAm. Moreover, the intensity of the low angle (1 0 0) and high angle peaks (110 and 200) decreased as compared with the parent carbon material (Fig. 2a). The large reduction in the intensity of XRD peaks was mainly due to the larger contrast in density between the carbon walls and the open pores relative to that between the carbon walls and the PNIPAAm molecule inside the pores. Thus the decrease in intensity did not mean a severe loss of structural order, which was further confirmed by TEM images (Fig. 3b). This

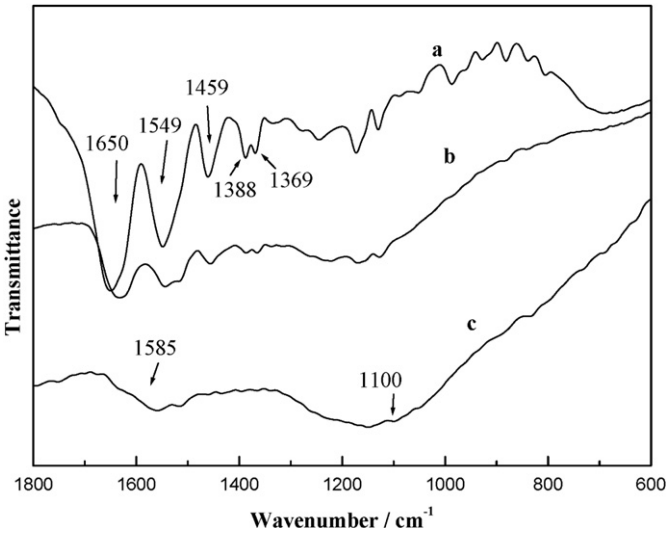

Fig. 1. IR spectra of PNIPAAm (a), PNIPAAm/OMCs composite (b) and pure carbon (c).

observation was consistent with the result obtained by Zhu et al. [6] and Vinu et al. [12].

Wide angle XRD patterns of the pure carbon material and PNIPAAm/OMCs composite both showed two broad diffraction peaks at about 23° and 43° for carbon material and the PNIPAAm/OMCs composite at the wide-angle range (10–60°) (the inset of Fig. 2), which could be indexed to the (0 0 2) and (1 0 1) diffraction for typical graphite-like carbon, respectively. In addition, no peak for bulk PNIPAAm ($2\theta = 13.5°$) [27] was observed for the PNIPAAm/OMCs composite, indicating that the encapsulated polymer was amorphous.

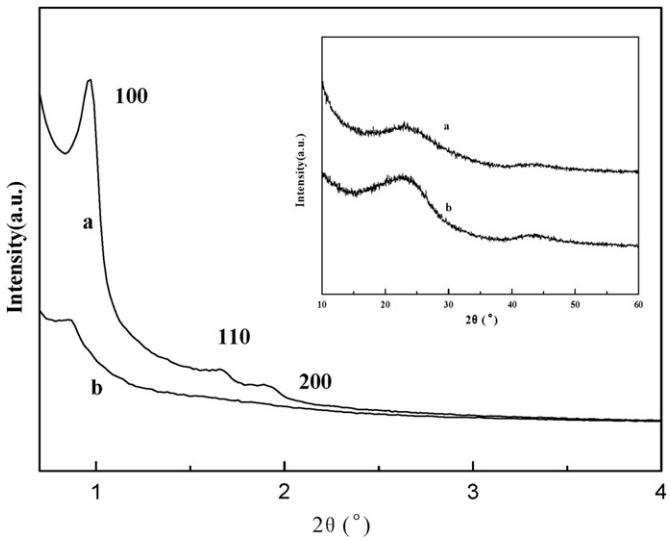

Fig. 2. Small-angle XRD patterns of the carbon (a) and the PNIPAAm/OMCs composite (b) (the inset figure was the wide angle patterns).

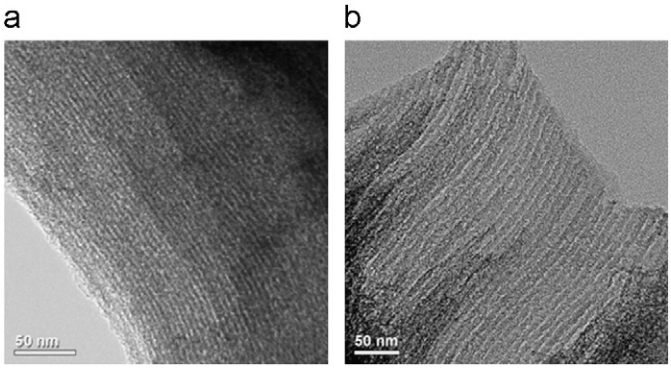

Fig. 3. TEM images of carbon material (a) and the PNIPAAm/OMCs composite (b).

The obvious hexagonal arrangement of mesopores was clearly observed (Fig. 3a), giving evidence for the presence of ordered mesopores and the carbon walls, which was consistent with the results of XRD analysis. For the PNIPAAm/OMCs composite, the ordered structure still remained and a little amount of polymers on the external surface of OMCs were observed (Fig. 3b).

The nitrogen sorption isotherms and pore size distributions of carbon material and the PNIPAAm/OMCs composite were shown in Fig. 4. The nitrogen sorption isotherms for parent carbon material (Fig. 4a) exhibited type IV curves with an obvious capillary condensation at a relative pressure p/p_0 0.4–0.7, indicating a uniform mesoporosity with a narrow pore size distribution. The calculation based on the isotherms showed that the pure carbon has a high BET surface area of 1006 m^2/g, a pore volume of 0.97 cm^3/g and a narrow pore size distribution at the mean value of 4.1.

The N_2 sorption isotherms of the PNIPAAm/OMCs composite (Fig. 4b) were also shown. Typical IV isotherms were obtained, indicating the reservation of a typical mesoporous material. Therefore, it could be deduced that the inclusion of PNIPAAm had not greatly changed the basic pore structure of the mesoporous carbons. The BET surface area, pore volume and pore size of the composite were 558 m^2/g, 0.54 cm^3/g and 4.0 nm, respectively. The BET surface area, pore volume and pore size showed a decrease after the inclusion of PNIPAAm. These results further proved that PNIPAAm had been successfully incorporated into the mesoporous channels. In addition, the composite showed high BET surface area and large pore volume, indicating its potential application as a host in storing more drug molecules and the drug-release system.

It could be observed (Fig. 5) that the endothermic peak of composite was at about 30.8 °C, lower temperature compared to that of pure PNIPAAm at about 33.7 °C. In addition, the temperature ranges of transition of composite were broader than that of pure PNIPAAm, which was due to the steric hindrance for conformation transition in confined geometries. This observation

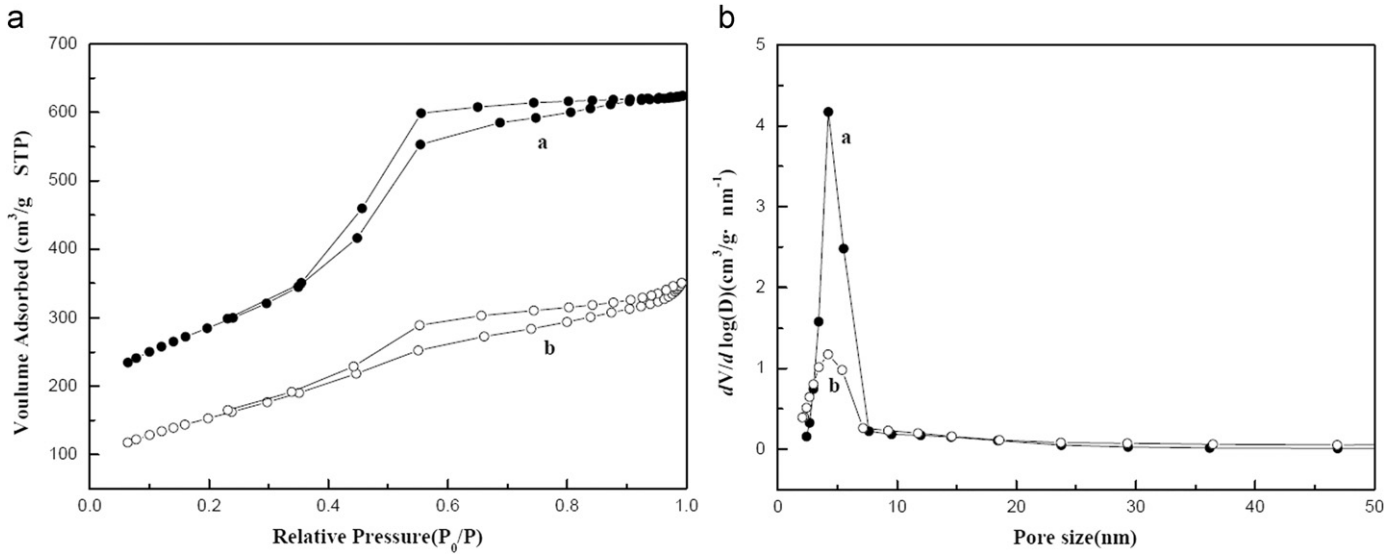

Fig. 4. N_2 sorption isotherms and pore size distribution of carbon material (a) and the PNIPAAm/OMCs composite (b).

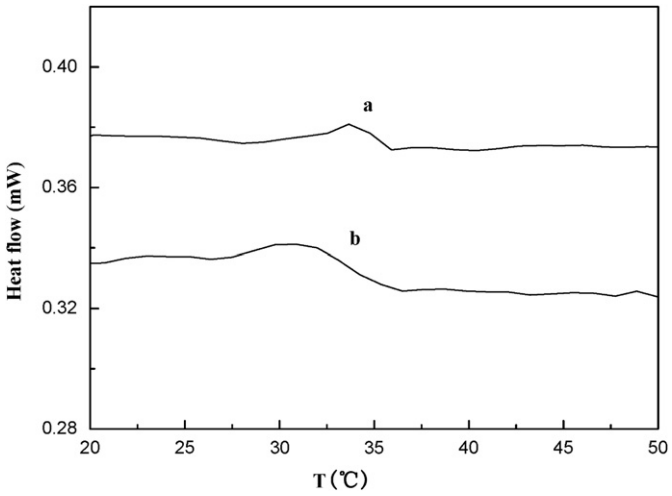

Fig. 5. DSC curves of pure PNIPAAm (a) and PNIPAAm/OMCs composite (b).

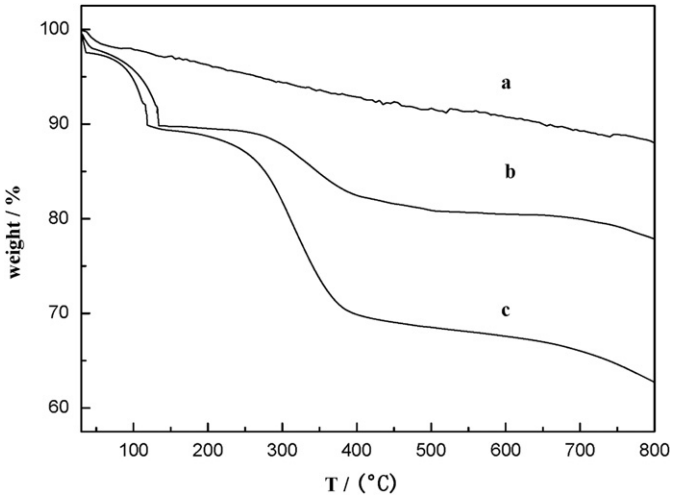

Fig. 6. TG curves of pure carbon (a), PNIPAAm/OMCs composite (b) and PNIPAAm/OMCs-IBU (c).

was consistent with the result obtained by Tian et al. [8], who reported DSC curves of PNIPAAm/SBA-15 composite.

For pure OMCs, a weight loss below 100 °C could be assigned to the loss of water molecules and no notable decrease in weight could be observed in the temperature range of 100–800 °C (Fig. 6).While the PNIPAAm/OMCs composite and PNIPAAm/OMCs-IBU, remarkable losses in weight was observed. The content of PNIPAAm in composite was 12% and the amount of IBU loaded onto the sample was 19% according to TG, respectively.

The amount of released IBU was 73% after 4 h at 37 °C, whereas only 25 wt% of the IBU was released after 6 h at 10 °C, and then almost no release happened from the system (Fig. 7). A more rapid release was also observed at 37 °C than at 10 °C, which further exhibited that the system could be performed for controlled delivery due to the temperature-responsive pattern. At temperatures below the LCST, PNIPAAm was in a water-swollen and extended state, which hampered IBU to diffuse from the channels. While at temperatures above the LCST, PNIPAAm was in a collapsed, hydrophobic state because the intramolecular hydrogen bonds between C═O and N–H groups in PNIPAAm chains were formed preferentially [1,8]. The drug molecules could be released from the pore channels.

In addition, UV spectra and high-performance liquid chromatography (HPLC) were investigated for pure ibuprofen (a) and the

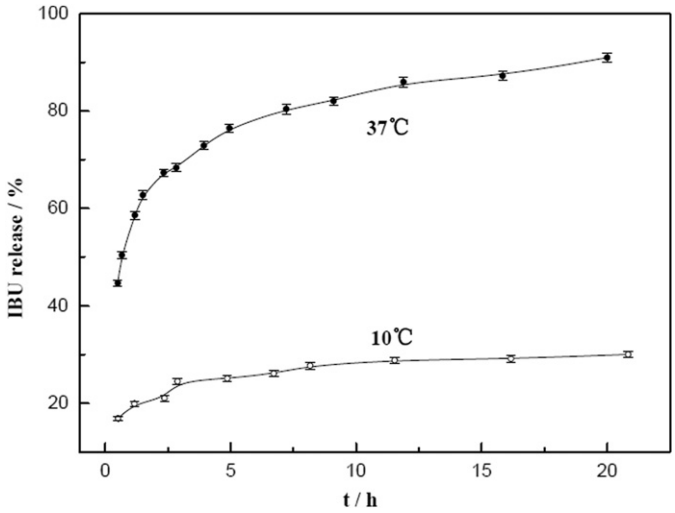

Fig. 7. IBU release plots from PNIPAAm/OMCs-IBU at 10 and 37 °C.

released ibuprofen (b) (**SEE Supporting information, Fig. S1**). The research results showed that the ibuprofen biomolecules are still viable after release.

4. Conclusions

A temperature-responsive PNIPAAm/OMCs composite was successfully synthesized by a simple wetness impregnation technique. The composite obtained possessed ordered hexagonal structure, high surface areas and pore volumes and the inclusion of PNIPAAm had not greatly changed the basic ordered pore structure of the OMCs. In vitro test of IBU release showed that the composite had the potential application in controlled drug delivery due to the temperature-responsive pattern.

Acknowledgments

The authors acknowledge the financial support from the National Science Foundation of China (No.50802017), the Medical Science Research Fund of GuangDong Province (No. B2009118) and the Teaching Staff Construction Fund of Guangdong Pharmaceutical University.

Appendix A. Supplementary Information

Supplementary data associated with this article can be found in the online version at doi:10.1016/j.jssc.2011.04.019.

References

[1] H.G. Schild, Prog. Polym. Sci. 17 (1992) 163–249.
[2] B. Menaa, F. Menaa, C. Aiolfi-Guimaraes, O. Sharts, Int. J. Nanotechnol. 7 (2010) 1–45.
[3] B. Menaa, Y. Miyagawa, M. Takahashi, M. Herrero, V. Rives, F. Menaa, D. Eggers, Biopolymers 91 (2009) 895–906.
[4] Q. Fu, R. Rama, T.L. Ward, Y. Lu, G.P. Lopez, Langmuir 23 (2007) 170–174.
[5] P.W. Chung, R. Kumar, M. Pruski, V.S.Y. Lin, Adv. Funct. Mater. 18 (2008) 1390–1398.
[6] S.M. Zhu, Z.Y. Zhou, D. Zhang, C. Jin, Z.Q. Li, Micropor. Mesopor. Mater. 106 (2007) 56–61.
[7] S.M. Zhu, Z.Y. Zhou, D. Zhang, Chem. Phys. Chem. 8 (2007) 2478–2483.
[8] B.S. Tian, C. Yang, J. Phys. Chem. C 113 (2009) 4925–4931.
[9] Y.F. Zhu, S. Kaskel, T. Ikoma, N. Hanagata, Micropor. Mesopor. Mater. 123 (2009) 107–112.
[10] A. Vinu, V. Murugesan, M. Hartmann, J. Phys. Chem. B 108 (2004) 7323–7330.

[11] A. Vinu, V. Murugesan, O. Tangermann, M. Hartmann, Chem. Mater. 16 (2004) 3056–3065.
[12] A. Vinu, M. Miyahara, K. Ariga, J. Phys. Chem. B 109 (2005) 6436–6441.
[13] X.F. Wang, P. Liu, Y. Tian, Micropor. Mesopor. Mater. 142 (2011) 334–340.
[14] J. Wang, J.D. Zhou, Z.S. Li, Y. He, S.S. Lin, Q. Liu, M.L. Zhang, Z.H. Jiang, J. Solid State Chem. 183 (2010) 2511–2515.
[15] L.M. Guo, L.X. Zhang, J.M. Zhang, J. Zhou, Q.J. He, S.Z. Zeng, X.Z. Cui, J.L. Shi, Chem. Commun. (2009) 6071–6073.
[16] S.B. Wang, Micropor. Mesopor. Mater. 117 (2009) 1–9.
[17] Y.F. Shi, Y. Wan, B. Tu, D.Y. Zhao, J. Phys. Chem. C 112 (2008) 112–116.
[18] Y.F. Zhu, J.L. Shi, Y.S. Li, H.R. Chen, W.H. Shen, X.P. Dong, Micropor. Mesopor. Mater. 85 (2005) 75–81.
[19] A.H. Lu, W. Schmidt, B. Spliethoff, F. Schuth, Adv. Mater. 15 (2003) 1602–1606.
[20] D.Y. Zhao, Q.S. Huo, J.L. Feng, B.F. Chmelka, G.D. Stucky, J. Am. Chem. Soc. 120 (1998) 6024–6036.
[21] T. Kokubo, H. Kushitani, S. Sakka, T. Kitsugi, T. Yamamuro, J. Biomed. Mater. Res. 24 (1990) 721–734.
[22] S.B. Cho, K. Nakanishi, T. Kokubo, N. Soga, C. Ohtsuki, T. Nakamura, T. Kitsugi, T. Yamamuro, J. Am. Ceram. Soc. 78 (1995) 1769–1774.
[23] C. Erbil, E. Kazancıoglu, N. Uyanık, Eur. Polym. J. 40 (2004) 1145–1154.
[24] W.G. Liu, B.Q. Zhang, W.W. Lu, X.W. Li, D.W. Zhu, K.D. Yao, Q. Wang, C.R. Zhao, C.D. Wang, Biomaterials 25 (2004) 3005–3012.
[25] P.A. Bazuła, A.H. Lu, J.J. Nitz, F. Schuth, Micropor. Mesopor. Mater. 108 (2008) 266–275.
[26] A. Sayari, B.H. Han, Y. Yang, J. Am. Chem. Soc. 126 (2004) 14348–14349.
[27] L. Ying, E.T. Kang, K.G. Neoh, J. Membr. Sci. 224 (2003) 93–103.